The new nitrogen dioxide (NO_2) linelist in the GEISA database

Journal of Molecular Spectroscopy 376 (2021)

A. Perrin [a], L. Manceron [b,c], J.-M. Flaud [d], F. Kwabia-Tchana [d], R. Armante [a], P. Roy [b], D. Doizi [e]

[a]Laboratoire de Météorologie Dynamique/IPSL, UMR CNRS 8539, Ecole Polytechnique, Université Paris-Saclay, Palaiseau Cedex, France;
[b]Sorbonne Université, CNRS, MONARIS, UMR 8233, 4 place Jussieu, Paris F-75005, France
[d]Laboratoire Inter-Universitaire des Systèmes Atmosphériques (LISA), UMR 7583, CNRS et Universités Paris Est et Paris Diderot, Institut Paul Simon Laplace, 94010 Créteil, France
[c] Ligne AILES, Synchrotron SOLEIL, L'Orme des Merisiers, St-Aubin BP48, 91192 Gif-sur-Yvette Cedex, France and MONARIS UMR 8233, CNRS-UPMC 75005, Paris, France.
Université Paris-Saclay, CEA, Service d'Etude du Comportement des Radionucléides, 91191 Gif-sur-Yvette, France
(e-mail: Raymond.armante@lmd.ipsl.fr, Agnes.Perrin@lmd.ipsl.fr,

We have generated new lists of line position, line intensity and line shape parameters of nitrogen dioxide ($^{14}N^{16}O_2$ and $^{15}N^{16}O_2$), here labeled as "GEISA-19", which have been included in the GEISA database (https://geisa.aeris-data.fr/). Except for the far infrared and the 13.3 µm regions, all spectral regions of the 1153–4775 cm^{-1} spectral domain are significantly modified by this major update of the GEISA linelist. For the 6.2 µm and 3.4 µm spectral regions, which correspond to the strongest absorption of NO_2, we proceed to a complete replacement of the lists for the first hot bands, $\nu_2+\nu_3-\nu_2$ and $\nu_1+\nu_2+\nu_3-\nu_2$, respectively, and to the inclusion, whenever possible, of higher order hot bands involving the (1,0,0), (0,2,0) and (0,0,1), (1,1,0), (2,0,0) or (0,0,2) states as lower states. Also, the $\nu_1+\nu_3$ linelist was improved for high rotational quantum numbers and the ν_3 and $\nu_1+\nu_3$ bands for $^{15}N^{16}O_2$, which is the second most abundant isotopologue of NO_2, are now included in the database. Finally several weak cold bands in the 2.2–4.9 µm region were added for the first time to the GEISA linelist. These new vibration rotation transitions were generated using existing literature data or making use of experimental data extracted from high resolution Fourier transform spectra recorded at SOLEIL for the purpose of this study. One outcome of this study was the first identification of the $\nu_1+2\nu_3-\nu_3$ hot band, leading to the first determination of the (1,0,2) energy level parameters. Also, an improved set of parameters was derived for the (0,1,1) state. The validation of the GEISA-19 linelist was performed through a detailed comparison at 296 K between computed and observed Fourier transform laboratory spectra. Also, the consistency, from one band to another, of the energy levels values was carefully checked. Finally inter-comparisons and verifications were performed using the recent versions of the HITRAN (https://hitran.org/) and HITEMP databases [R.J. Hargreaves, I. E. Gordon, L. S. Rothman, S. A. Tashkun, V. I. Perevalov, A. A. Lukashevskaya, S. N. Yurchenko, J. Tennyson, and H. S.P. Müller. JQSRT. 232 35 (2019)]. Our conclusions are that, at 296 K, GEISA-19 is of better quality than HITRAN2016-updated or HITEMP in the overall 1153–4775 cm^{-1} spectral region. As compared to its previous version, this new linelist will lead to an improved quality of the NO_2 retrievals that will be performed for the future IASI-NG (Infrared Atmospheric Sounding Interferometer New Generation) satellite instrument (https://iasi-ng.cnes.fr/fr). However, contrary to HITEMP, GEISA-19 which does not include transitions involving high rotational quantum numbers or belonging to very high order hot bands cannot be used for hot temperature conditions

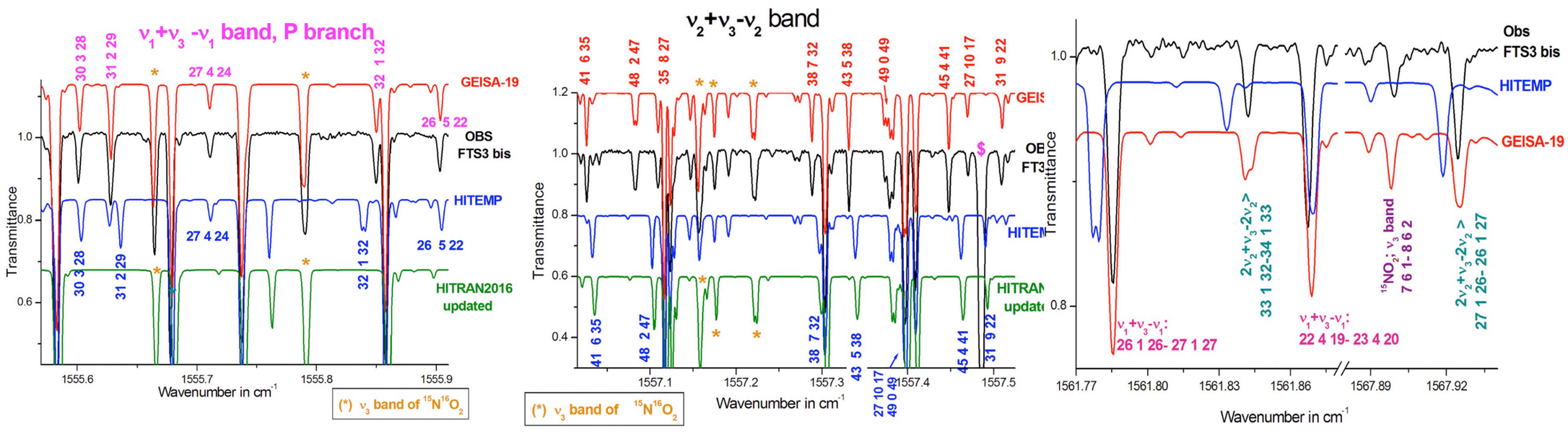

Portions of the P- branch of the ν_3 band in the 1555.7 cm^{-1} , 1557 cm^{-1} and 1561–1568 cm^{-1} spectral ranges. The GEISA-19, HITEMP, and HITRAN2016-updated linelists are compared.

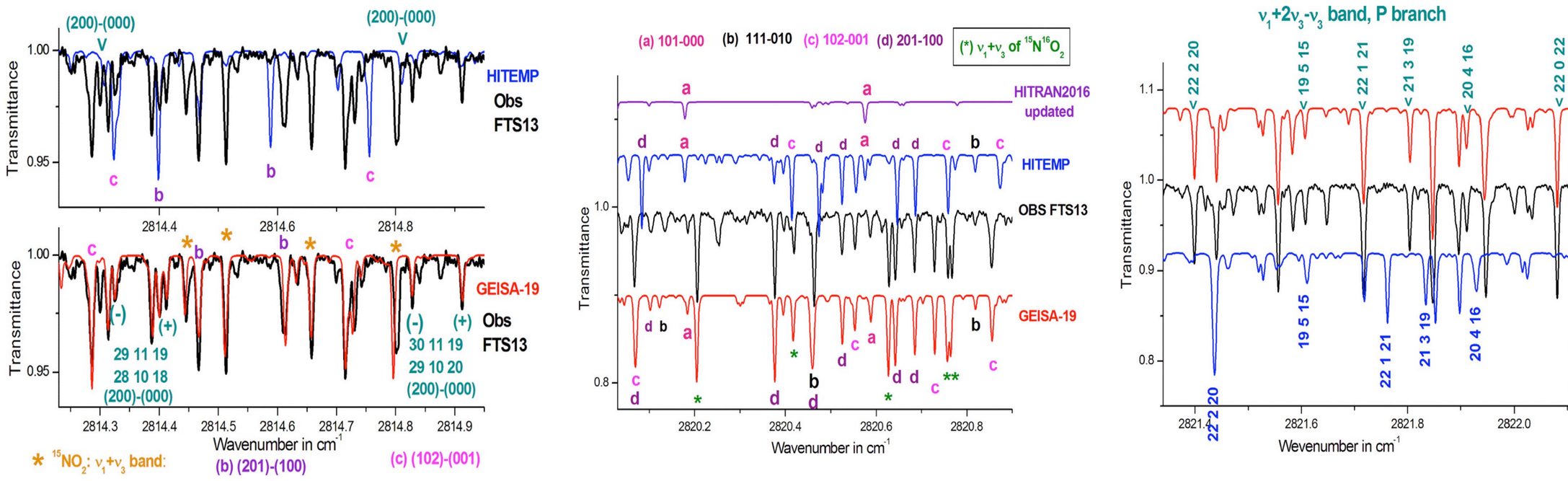

Portions of the P branch of the $\nu_1+\nu_3$ band in the 2814.4 cm^{-1} , 2820 cm^{-1} and 2821 cm^{-1} regions. The GEISA-19, HITEMP, and HITRAN2016-updated linelists are compared.

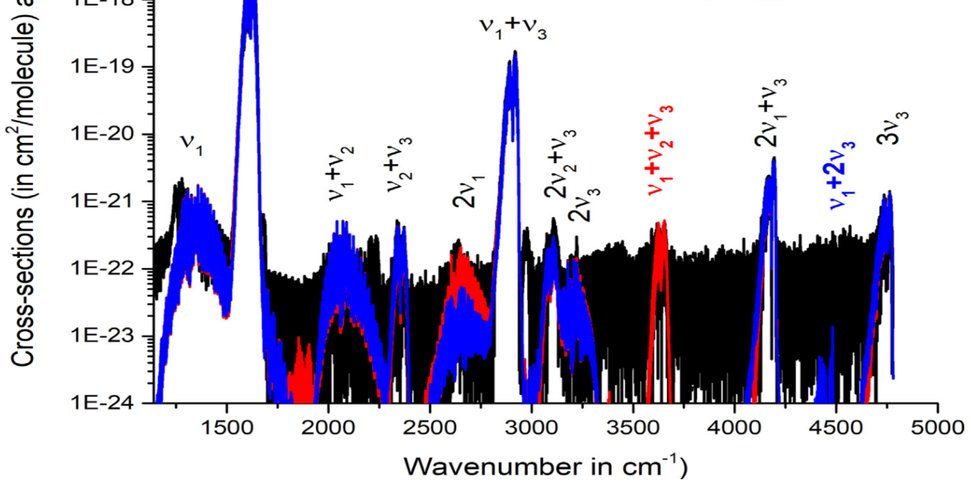

The PNNL cross sections for NO_2 (NO2_25T). Comparison with the computed cross sections using the GEISA-19 and HITEMP databases.

Description of the GEISA-19 database (1153–4775.4 cm-1)

The $^{14}N^{16}O_2$ linelist:

V'	V''	Nb	Centre	S_min	S_max	Band Int	Int_{Min}	Int_{Max}
101	001	966	1289.89	1224.94	1607.29	0.185E−22	0.10E−25	0.59E−25
100	000	8145	1319.79	1153.01	1664.24	0.721E−19	0.10E−24	0.17E−21
101	020	2	1408.40	1508.14	1615.42	0.204E−25	0.10E−25	0.10E−25
220	200	5	1473.24	1530.94	1582.85	0.285E−24	0.14E−25	0.11E−24
021	001	239	1475.63	1533.53	1621.31	0.450E−21	0.11E−24	0.49E−23
130	110	78	1483.98	1533.70	1605.43	0.132E−23	0.10E−25	0.73E−25
120	100	520	1485.81	1455.08	1652.23	0.230E−22	0.10E−25	0.16E−24
040	020	256	1494.66	1545.26	1631.78	0.140E−20	0.10E−24	0.20E−22
030	010	1927	1496.39	1429.25	1690.68	0.761E−21	0.20E−25	0.16E−22
020	000	4426	1498.34	1369.96	1800.30	0.645E−19	0.10E−24	0.61E−21
201	200	1659	1552.60	1503.90	1586.05	0.150E−21	0.10E−25	0.36E−24
003	002	850	1552.77	1516.38	1581.14	0.244E−22	0.10E−25	0.66E−25
102	101	1350	1554.12	1510.73	1586.95	0.765E−22	0.10E−25	0.18E−24
111	110	3073	1574.72	1509.97	1614.74	0.238E−20	0.10E−25	0.56E−23
002	001	3147	1584.59	1517.86	1626.60	0.432E−19	0.10E−24	0.99E−22
101	100	4383	1586.95	1504.16	1667.57	0.909E−19	0.10E−25	0.21E−21
021	020	3032	1594.14	1526.69	1635.95	0.351E−19	0.10E−24	0.88E−22
011	010	6947	1605.50	1505.60	1752.36	0.145E−17	0.20E−25	0.34E−20
001	000	10,856	1616.85	1429.63	1835.38	0.569E−16	0.10E−24	0.13E−18
002	020	243	1703.10	1525.53	1616.92	0.314E−21	0.10E−24	0.36E−23
002	100	880	1881.65	1754.08	1953.09	0.186E−21	0.10E−24	0.72E−24
110	000	7593	2063.12	1921.88	2346.16	0.165E−19	0.10E−25	0.41E−22
011	000	2551	2355.15	2289.98	2395.03	0.850E−20	0.50E−25	0.23E−22
200	000	5982	2627.34	2457.95	2921.80	0.839E−20	0.50E−25	0.23E−22
130	010	293	2797.45	2826.76	2924.89	0.671E−22	0.51E−25	0.23E−23
120	000	1531	2805.60	2740.02	3023.06	0.853E−21	0.50E−25	0.53E−23
102	001	1836	2844.01	2787.39	2872.69	0.217E−20	0.10E−24	0.51E−23
201	100	3245	2860.14	2790.47	2888.91	0.923E−20	0.50E−26	0.22E−22
111	010	3904	2888.19	2811.08	2919.85	0.734E−19	0.51E−25	0.17E−21
101	000	8731	2906.74	2688.75	3148.79	0.287E−17	0.50E−25	0.66E−20
040	000	194	2993.00	3040.81	3133.67	0.257E−21	0.11E−24	0.37E−23
021	000	2512	3092.48	3032.58	3283.84	0.650E−20	0.10E−24	0.15E−22
002	000	3597	3201.44	3019.48	3322.09	0.377E−20	0.10E−24	0.14E−22
210	000	1018	3364.57	3291.70	3658.07	0.215E−22	0.10E−25	0.15E−24
130	000	275	3547.10	3581.21	3678.91	0.110E−22	0.10E−25	0.36E−24
111	000	3999	3637.84	3563.65	3690.60	0.123E−19	0.10E−25	0.28E−22
220	000	333	4100.58	4100.56	4207.21	0.191E−21	0.50E−25	0.58E−22
201	000	4234	4179.94	4087.83	4230.50	0.790E−19	0.50E−25	0.18E−21
022	000	133	4656.34	4702.20	4768.40	0.145E−22	0.50E−25	0.18E−24
003	000	3647	4754.21	4624.75	4775.31	0.304E−19	0.50E−25	0.70E−22

The $^{15}N^{16}O_2$ linelist

V_U	V_L	Nb	Band center	S_{Min}	S_{Max}	Band Int	Int_{Min}	Int_{Max}	Ca N
001	000	5860	1582.10	1500.73	1660.45	2.039E−19	2.00E−26	4.56E−22	77
120	000	157	2761.21	2819.67	2889.29	0.162E−22	0.21E−25	0.21E−24	42
101	000	3640	2858.71	2784.88	2890.81	1.036E−20	3.64E−28	2.34E−23	61

Total: 118,249 lines

References

[1] N. Jacquinet-Husson, R. Armante, N.A. Scott, A. Chedin, *et al.* JQSRT 327, 31–72 (2016); T.Delahaye, R.Armante, N.A.Scott, N.Jacquinet-Husson, A.Chédin, *et al.* J. Mol. Spectrosc. **380**, 2021
[2] I.Gordon *et al*. JQSRT 203, 3–69 (2017); JQSRT 277 (2022)
[3] R.J. Hargreaves, I.E. Gordon, L.S. Rothman, S.A. Tashkun, V.I. Perevalov, A.A. Lukashevskaya, S.N. Yurchenko, J. Tennyson, H.S.P. Müller, JQSRT 232 (2019) 35–53.
18] A. Perrin, L. Manceron, F. Kwabia Tchana, Mol. Phys. 118 (2020)
[36] S. Sharpe, T. Johnson, R. Sams, P. Chu, G. Rhoderick, P. Johnson, Appl. Spectrosc. 58 (2004) 1452–1461.

The authors thank the AERIS atmospheric and data pole and the CNES French space agency to make available the IASI level 1 data. Work also supported by the French National programme ANR (ANR-19-CE29-0013) 'QUASARS' .